

# 000 001 002 003 004 005 006 007 008 009 010 011 012 013 014 015 016 017 018 019 020 021 022 023 024 025 026 027 028 029 030 031 032 033 034 035 036 037 038 039 040 041 042 043 044 045 046 047 048 049 050 051 052 053 NOT ALL BITS ARE EQUAL: HOW MODEL SCALE CHANGES MEMORY-OPTIMAL REASONING

Anonymous authors

Paper under double-blind review

## ABSTRACT

While 4-bit quantization has emerged as a memory-optimal choice for non-reasoning models and zero-shot tasks across scales, we show that this universal prescription fails for reasoning models, where KV cache rather than model size can dominate memory. Through systematic experiments on mathematical, [code generation](#), and knowledge-intensive reasoning tasks, we find a *scale-dependent trade-off*: models with an effective size below 8-bit 4B parameters achieve better accuracy by allocating memory to larger weights, rather than longer generation, while larger models benefit from the opposite strategy. This scale threshold also determines when parallel scaling becomes memory-efficient and whether KV cache eviction outperforms KV quantization. Our findings show that memory optimization for LLMs cannot be scale-agnostic, while providing principled guidelines: for small reasoning models, prioritize model capacity over test-time compute, while for large ones, maximize test-time compute. Our results suggest that optimizing reasoning models for deployment requires fundamentally different strategies than those established for non-reasoning ones.

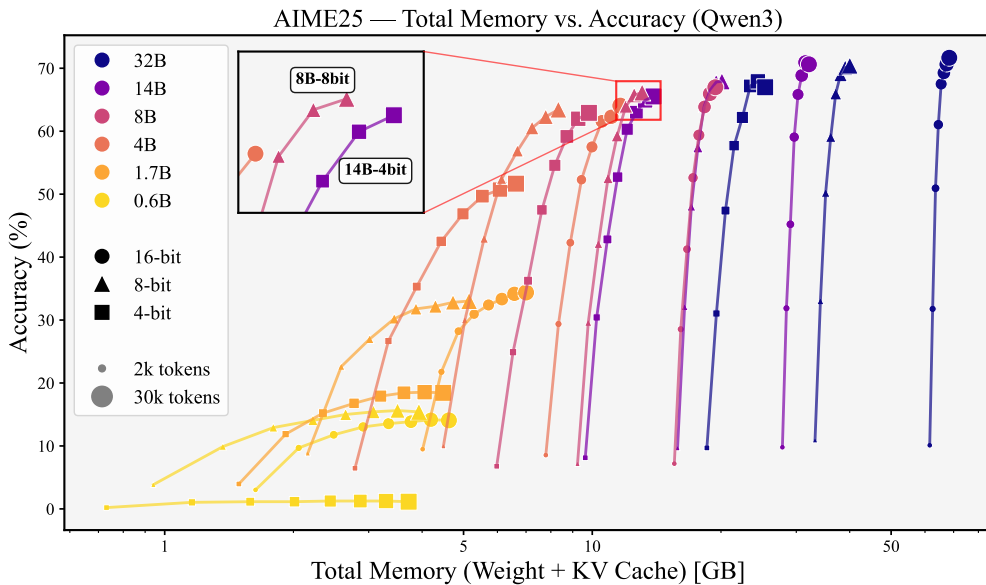


Figure 1: **Memory vs. Accuracy for serial test-time scaling on AIME25.** The plot illustrates the trade-off between pass@1 accuracy and total memory (weight + KV cache) for the Qwen3 family. Model weights are quantized to 8-/4-bit using GPTQ. Along each curve, the KV cache grows as the generation length is increased via budget forcing. For models effectively smaller than an 8-bit 4B, increasing the token budget to saturation is memory-inefficient. Furthermore, for mathematical reasoning, higher weight precision (16-/8-bit) proves more memory-efficient than 4-bit.

054 

## 1 INTRODUCTION

055  
 056 Prior memory–performance trade-off studies on Large Language Models (LLMs) for non-reasoning  
 057 models have focused mostly on compressing model weights, since the model weight generally con-  
 058 sumes far more GPU memory than the Key-Value (KV) cache memory (Dettmers & Zettlemoyer,  
 059 2023; Frantar et al., 2022; Lin et al., 2024). Modern reasoning models, however, generate substan-  
 060 tially more tokens, causing the proportionally increasing KV cache to become a significant bottle-  
 061 neck. For instance, a Qwen3-4B model at 4-bit weights occupies 2.49 GB, but its KV cache for a  
 062 32k-token generation requires 4.42 GB ( $\approx 1.8 \times$  the weights). With the KV cache becoming a dom-  
 063 inant component of memory, it is unclear whether the results established for non-reasoning models  
 064 still hold for long-generation reasoning tasks.

065 In this work, we aim to investigate the general principles of memory compression for reasoning  
 066 models. In addition to the conventional factors of model size and weight precision, our analysis in-  
 067 corporates three other factors that distinctly affect memory–accuracy trade-offs to reasoning models:  
 068 generation length, parallel scaling, and KV cache compression. Overall, we ask the question:

069 *Under a fixed memory budget, how should one navigate the trade-offs between **model size, weight**  
 070 **precision, token budget, sample size for parallel scaling, and KV cache compression**  
 071 **to maximize performance for reasoning models?***

072 We conduct an empirical study mainly focusing on the Qwen3 model family (0.6B to 32B) (Yang  
 073 et al., 2025) across four benchmarks: AIME25, GPQA-Diamond, [LiveCodeBench](#), and [MATH500](#).  
 074 Furthermore, we evaluate the DeepSeek-R1-Distill (Guo et al., 2025) and OpenReasoning-  
 075 Nemotron (Majumdar et al., 2025) reasoning model families to verify that our main findings  
 076 from Qwen3 generalize beyond a single model family. Our investigation spans over **1,700** dif-  
 077 ferent scenarios, exploring 4-bit and 8-bit GPTQ weight quantization (Frantar et al., 2022), rea-  
 078 soning token budgets from 2k to 30k, parallel scaling via majority voting with up to 16 sam-  
 079 ples, and two approaches to KV cache compression: eviction, using R-KV (Cai et al., 2025) and  
 080 StreamingLLM (Xiao et al., 2023b), and quantization with HQQ (Badri & Shaji, 2023). While our  
 081 findings do not provide specific prescriptions for all tasks or models, we provide general principles  
 082 to consider for memory-efficient reasoning models with minimal loss of accuracy.

083 **Our contributions.** In Section 4, we investigate how to allocate memory between model weights  
 084 and the KV cache under serial test-time scaling. For example, which will achieve higher accuracy:  
 085 a 32B 8-bit LLM with less KV cache (*i.e.*, less test-time compute), or a 32B 4-bit LLM with more  
 086 KV cache? We find that there is *no* optimal strategy that is universal across scale: for models with  
 087 effective size (parameters  $\times$  bits per weight) below 8-bit 4B, allocating more memory to model  
 088 weights yields larger gains, whereas above this threshold, memory is better spent increasing the  
 089 test-time budget until performance saturates.

090 We also discover that the choice of weight precision depends on the nature of the task. For  
 091 knowledge-intensive reasoning, 4-bit weight quantization is broadly memory-optimal, consistent  
 092 with established findings on the effectiveness of 4-bit or lower precision for zero-shot, non-reasoning  
 093 models (Dettmers & Zettlemoyer, 2023; Frantar et al., 2022; Chee et al., 2023). For mathematical  
 094 reasoning and code generation tasks, however, the higher fidelity of 8 or 16-bit model weights with  
 095 smaller KV cache often provides stronger performance, suggesting that intricate computational tasks  
 096 are more sensitive to loss in precision.

097 Orthogonal to longer generations, increasing the number of generations can yield substantial  
 098 gains (Brown et al., 2024), yet its memory efficiency remains under-explored. Parallel scaling via  
 099 majority voting on top of serial scaling introduces another trade-off: a larger KV cache propor-  
 100 tional to group size for higher accuracy. This strategy is only more memory-efficient than serial  
 101 scaling for models with an effective size at or above 8-bit 4B. Interestingly, for such models, the  
 102 memory-optimal group size also increases with the total memory budget. **Moreover, we show that**  
 103 **using an external verifier such as Process Reward Model (PRM) is memory-inefficient compared to**  
 104 **self-contained majority voting.**

105 In Section 5, we investigate how KV cache compression affects the memory–accuracy trade-off by  
 106 considering both KV cache eviction and quantization methods. Across model sizes and weight pre-  
 107 cisions, both eviction and quantization advance their Pareto frontiers beyond the baseline without

108 cache compression. The choice of compression method should be dictated by effective size: eviction  
 109 offers a better memory trade-off for small models (effective size below 8-bit 4B), while both  
 110 strategies are competitive for larger models.

111 Overall, the memory-optimal strategy for reasoning models is *not* universal, but is instead mainly  
 112 governed by the model’s effective size. We summarize our main empirical findings as follows:  
 113

- 114 1. For models effectively smaller than 8-bit 4B, it is more memory-efficient to allocate mem-  
 115 ory to larger weights than to longer generations, while larger models benefit more from  
 116 longer generations.
- 117 2. 4-bit weights are broadly memory-optimal for knowledge-intensive tasks, while 8-bit or  
 118 16-bit weights are more memory-efficient for mathematical reasoning **and code generation**.
- 119 3. Parallel scaling only improves the memory–accuracy trade-off for models effectively larger  
 120 than 8-bit 4B. The memory-optimal group size increases with the memory budget.
- 121 4. Weight quantization alone is not sufficient for memory-optimal reasoning; compressing the  
 122 KV cache leads to more memory-efficient reasoning.
- 123 5. KV cache eviction provides a better memory–accuracy trade-off than KV cache quantiza-  
 124 tion for models with an effective size smaller than an 8-bit 4B model.

## 127 2 BACKGROUND

128 **Weight-only quantization.** Weight-only post-training quantization replaces full-precision  
 129 weights with low-bit representations without retraining, reducing memory usage. Weight-only quantiza-  
 130 tion allows lower bit-widths compared with weight activation quantization, as it is more robust  
 131 to quantization error (Yao et al., 2023). However, weight-only quantization requires dequantization  
 132 before multiplying with activations, so it does not reduce computational cost during inference. Any  
 133 speed-up instead comes from reduced memory movement. In this work, we adopt GPTQ (Frantar  
 134 et al., 2022), a weight-only quantization method that minimizes layer-wise quantization error using a  
 135 small calibration set, updating weights using inverse-Hessian information. **We additionally replicate**  
 136 **key experiments using AWQ (Lin et al., 2024) and FP8 (Micikevicius et al., 2022) to verify that our**  
 137 **conclusions do not depend on a specific quantization scheme.**

138 **KV cache quantization.** KV cache quantization stores key and value tensors at reduced precision  
 139 to lower memory footprint and memory bandwidth during decoding. Unlike weight-only quantiza-  
 140 tion, KV quantization is applied online at inference. During prefill, the KV tensors for the entire  
 141 input context are quantized and cached in low precision. During decode, the cached tensors are  
 142 dequantized on the fly for attention computations. Prior works conventionally maintain a small  
 143 full-precision buffer for the most recent tokens, appending new key and value tensors to this buffer  
 144 during decoding. In this work, we use per-channel symmetric quantization of both keys and values  
 145 with an HQQ backend (Badri & Shaji, 2023). HQQ is a fast, calibration-free quantization method,  
 146 making it particularly well-suited for online KV cache quantization.

147 **KV cache eviction.** On the other hand, KV cache eviction has also emerged as a critical optimiza-  
 148 tion strategy, reducing KV cache size and the cost of attention computation. Specifically for reason-  
 149 ing models, we consider dynamic eviction policies that continuously update the KV cache during  
 150 decoding. Early work, such as StreamingLLM (Xiao et al., 2023b), employs a sliding-window mech-  
 151 anism that preserves the most recent key and value tensors, in addition to the initial sequence tokens  
 152 known as the attention sink. More recently, R-KV (Cai et al., 2025) proposes redundancy-aware  
 153 selection for reasoning models: it estimates token importance and redundancy during decoding and  
 154 jointly selects non-redundant, informative tokens to retain, reporting near-baseline accuracy with a  
 155 small fraction of the KV cache. In Section 5, we study how these eviction policies, together with  
 156 KV cache quantization, shift the trade-off frontiers.

157 **Test-time scaling.** We scope this work to test-time scaling methods that do not rely on exter-  
 158 nal models such as verifiers or process reward models. Reasoning models are typically trained to  
 159 produce extended chain-of-thought, continuing generation with planning and reflection to improve  
 160 performance (Guo et al., 2025; Jaech et al., 2024; Yang et al., 2025). We refer to this as serial

162 scaling. Muennighoff et al. (2025) introduces budget forcing to scale serial responses beyond the  
 163 model’s natural length for higher accuracy. When the model attempts to stop, a short cue is appended  
 164 to continue decoding to a specified token budget. Another line of work, parallel scaling, generates  
 165 multiple independent reasoning trajectories (Brown et al., 2024). In its simplest form, without any  
 166 external model, majority voting selects the final answer as the most frequent among the indepen-  
 167 dently sampled outputs (Wang et al., 2022). Further related work is discussed in Appendix A.

### 169 3 EXPERIMENTAL SETUP

171 Given the practical challenge of balancing performance against memory usage, we now formalize  
 172 the problem of selecting an optimal configuration under a fixed memory budget. Specifically, we  
 173 solve the following selection problem

$$175 \quad \arg \max_{(N, P_W, \pi_{kv}, T, G)} \text{Acc}_t(N, P_W, \pi_{kv}, T, G) \quad \text{s.t.} \quad C_{\text{mem}} \leq B_{\text{mem}},$$

177 Here, configurations  $(N, P_W, \pi_{kv}, T, G)$  specify the number of parameters, weight precision, KV  
 178 strategy (quantization or eviction), test-time token budget, and sampling group size ( $G > 1$  indicates  
 179 multiple samples for majority voting), respectively.  $C_{\text{mem}}$  represents the total memory cost, and  
 180  $B_{\text{mem}}$  is the specified memory budget.

181 The memory cost is given by

$$183 \quad C_{\text{mem}} = M_{\text{weights}}(N, P_W) + M_{\text{kv}}(N, \pi_{kv}, T, G).$$

185 Here  $M_{\text{weights}}$  is the memory footprint of the weights, roughly proportional to  $N \cdot P_W$ . Note that  
 186 throughout the paper, we use *model size* to refer to the number of parameters  $N$  and *effective size*  
 187 or *scale* for the memory footprint of the weights,  $M_{\text{weights}}$ .  $M_{\text{kv}}$  is KV cache memory, which is  
 188 roughly proportional to  $N, G$ , and  $T$ , except with  $\pi_{kv} = \text{eviction}$ , where the cost becomes constant  
 189 beyond a certain token budget. Please refer to Appendix B for the exact memory cost equations and  
 190 model-specific values.

191 **Models.** We experiment with the Qwen3 model family (Yang et al., 2025), which spans from  
 192 0.6B to 32B parameters, offering a wide range of model sizes and thus making it well-suited for a  
 193 fine-grained systematic study across scales. [We additionally evaluate the DeepSeek-R1-Distill \(Guo et al., 2025\) and OpenReasoning-Nemotron \(Majumdar et al., 2025\) reasoning model families to test whether our findings generalize beyond Qwen3.](#)

197 **Tasks.** Experiments are conducted on challenging benchmarks representing complementary diffi-  
 198 culty profiles. AIME25 (AIME, 2025) is a competition-level mathematical benchmark that stresses  
 199 multi-step reasoning, and [MATH500 \(Lightman et al., 2023\) extends this to a larger, more diverse math set](#). In contrast, GPQA-Diamond (Rein et al., 2024) emphasizes scientific knowledge and in-  
 200 tegrated reasoning across domains such as chemistry, biology, and physics (Li et al., 2025b), while  
[LiveCodeBench \(Jain et al., 2024\) evaluates reasoning in code generation](#).

204 **Inference details.** Unless otherwise specified, we report accuracy averaged over 32 genera-  
 205 tions per instance and sample with temperature 0.6. Following Muennighoff et al. (2025), for  
 206 serial scaling with budget forcing, if generation terminates earlier than the desired token bud-  
 207 get, we replace the end-of-sequence token with the prompt `Wait` and continue decoding until  
 208 the target budget is reached. When the desired budget is met, we inject the prompt `**Final`  
 209 `Answer**\n\boxed{}`. We evaluate token budgets from 2k to 30k in 4k increments. We plan to  
 210 release our code publicly.

### 212 4 TEST-TIME SCALING WITH WEIGHT-ONLY QUANTIZATION

214 *When aiming for the best performance under limited memory, how should memory be allocated  
 215 between model weights and KV cache? Additionally, when allocating space for model weights, is it  
 better to use more parameters at lower precision or fewer parameters at higher precision?*

To answer these questions, we study test-time scaling across different model sizes ( $N$ ) and weight precisions ( $P_W \in \{4, 8, 16\}$ ) by varying the test-time token budget ( $T$ ). We use GPTQ to quantize models into 4-bit and 8-bit precisions. For this analysis, we fix  $\pi_{kv}$  to keep all cache entries (no eviction, full precision) and first present results for a sampling group size of  $G = 1$ . We later discuss parallel scaling with  $G > 1$  and other  $\pi_{kv}$  policies.

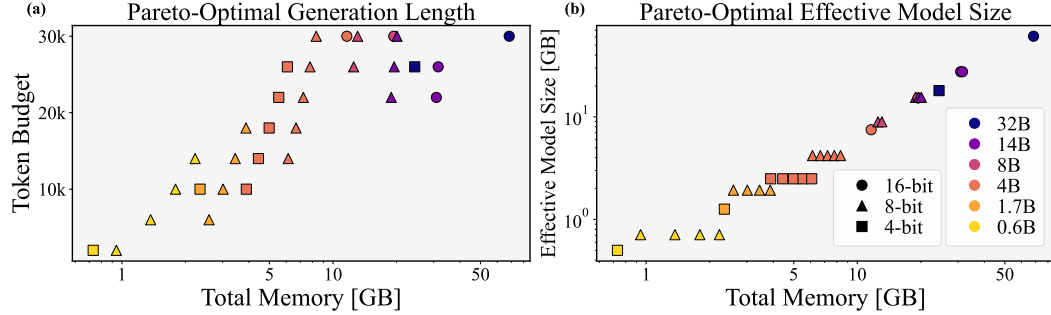


Figure 2: **Composition of Pareto-optimal configurations (AIME25, Qwen3).** The token budget (a) and effective model size (b) are plotted against the total memory budget for configurations on the Pareto frontier from Figure 1. The plots illustrate a strategic shift: at lower memory budgets ( $< 10$  GB), increasing effective model size is memory-efficient, whereas at higher budgets, increasing the token budget becomes the dominant strategy for improving performance.

Figure 1 reveals the Pareto frontier for accuracy versus total memory under serial scaling with a full-precision KV cache. Analyzing the configurations that lie on this frontier provides practical recommendations for optimizing model selection, weight precision, and test-time budgets within fixed memory constraints:

**For models effectively smaller than 8-bit 4B, memory is better spent on increasing the effective model size rather than increasing the test-time budget until saturation.** While extending the generation budget of a small model is often viewed as a way to trade higher latency for lower memory usage compared to using a large model, our analysis reveals this is a false economy. In fact, for models effectively smaller than 8-bit 4B, this strategy is often suboptimal in total memory. Figure 2 shows that for memory budgets below 8 GB, the Pareto frontier is advanced primarily by increasing model size, not the token budget. For instance, the 1.7B model in 8-bit with a 6k token budget outperforms the 0.6B model in 8-bit with an 18k token budget. Similarly, the 4B model in 4-bit with a 10k token budget surpasses the 1.7B model in 8-bit with an 18k token budget, demonstrating that choosing a model with a larger effective size is better under a similar memory budget. As our latency analysis confirms (Appendix C.1), these configurations with larger effective sizes are also faster because end-to-end latency is dominated by the token budget, making the choice to increase the model’s effective size strictly dominant.

**For large models with an effective size at or above 8-bit 4B, memory is more efficiently used when increasing the test-time budget until performance saturates.** In direct contrast to the strategy for small models, extending the generation budget is a more memory-efficient way to improve accuracy for large models. This strategic shift is clearly illustrated in Figure 2, where for memory budgets larger than 10 GB, the best-performing configurations on the Pareto frontier consistently feature token budgets above 20k. In this regime, increasing the token budget becomes the dominant method for improving accuracy.

We further confirm that our conclusions about weight precision are not tied to GPTQ. In Appendix C.2, we show that AWQ and FP8 weight quantization yield nearly identical memory-accuracy curves to GPTQ (Figure 12), and that the observed trends are robust across quantization schemes. Separately, while the above analysis assumes a scenario where each inference instance uses the entire model and KV cache, in practice, model weights can be amortized across multiple concurrent generations, fundamentally changing the memory dynamics; Appendix C.3 analyzes this setting under different theoretical batch sizes.

270

271

272

273

274

275

276

277

278

279

280

281

282

283

284

285

286

287

288

289

290

291

292

293

294

295

296

297

298

299

300

301

302

303

304

305

306

307

308

309

310

311

312

313

314

315

316

317

**Finding 1**

The memory-efficient allocation strategy between model weights and KV cache is scale-dependent. For models effectively smaller than 8-bit 4B, memory is more efficiently allocated to increasing the effective model size. For models at or above this threshold, it becomes more memory-efficient to increase the test-time budget until performance saturates.

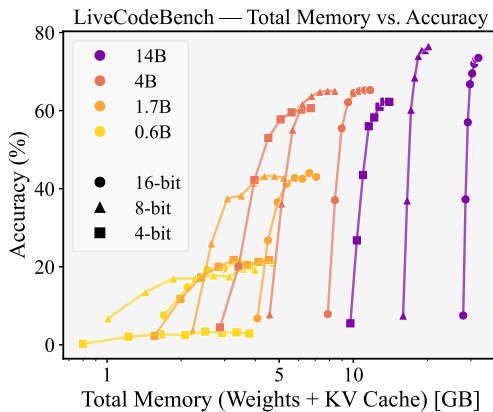


Figure 3: **Memory vs. Accuracy on LiveCodeBench (Qwen3).** Higher precision (8-/16-bit) remains more memory-efficient than 4-bit. The memory-optimal strategy shifts from favoring model weights at small budgets to longer generations at larger budgets.

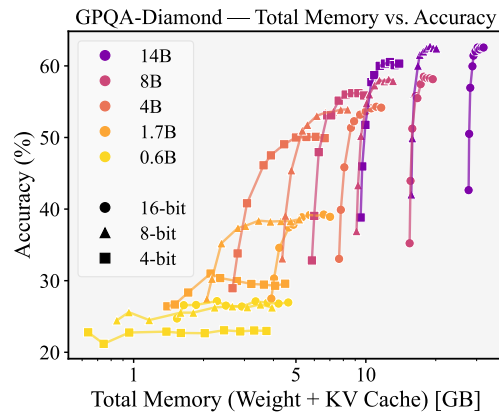


Figure 4: **Memory vs. Accuracy on GPQA-Diamond (Qwen3).** Unlike mathematical reasoning and code generation, 4-bit weights remain broadly memory-optimal for this knowledge-intensive task across memory budgets.

**The memory-optimal weight precision is task- and size-dependent.** Our findings show that for mathematical reasoning tasks, 4-bit weight quantization is consistently memory-inefficient. On the AIME25 benchmark, 8-bit is memory-optimal for small models ( $N \in \{0.6B, 1.7B\}$ ), as the performance gains from reallocating memory saved by 4-bit quantization to a larger token budget are insufficient to compensate for the accuracy loss. This inefficiency of 4-bit persists at larger  $N$ , where 8-bit and 16-bit configurations achieve higher accuracy at comparable memory. This is shown in Figure 2 (b), where 8-bit or 16-bit weights are most often memory-optimal along the frontier for memory budgets larger than 6 GB. Notably, the 8B model in 8-bit consistently outperforms the 14B model in 4-bit (Figure 1), and the 32B model in 4-bit is strictly dominated by both the 14B model in 8-bit and the 8B model in 16-bit. Such findings are in direct contrast to Dettmers & Zettlemoyer (2023). **LiveCodeBench** exhibits a similar preference for higher weight precision over 4-bit (Figure 3), and we refer to Appendix C.4 for a detailed analysis of LiveCodeBench and **MATH500**. However, we do find that for knowledge-intensive tasks, 4-bit quantization is broadly memory-optimal. As shown in Figure 4 for GPQA-Diamond, the frontier shifts to favor lower precision. This suggests that different task types place different demands on model parameters. Mathematical reasoning may rely on numerical precision within the weights, which is damaged by aggressive 4-bit quantization. On the other hand, knowledge-intensive tasks prioritize maximizing the number of parameters to increase knowledge capacity, making 4-bit large models more memory-efficient.

**Finding 2**

For knowledge-intensive tasks, 4-bit is broadly memory-optimal. For mathematical reasoning and code generation tasks, higher precision is required. 8-bit is memory-optimal for small models ( $N \in \{0.6B, 1.7B\}$ ), while both 8-bit and 16-bit are competitive at larger numbers of parameters.

In addition to serial scaling by increasing the token budget, we can introduce a parallel scaling axis by increasing the sampling group size ( $G$ ). Assuming a batched inference setting, the KV cache grows with  $G$ , in exchange for higher accuracy. This raises another key question:

*When is it more memory-efficient to allocate memory to parallel samples, versus allocating it to a larger effective model size or a longer token budget?*

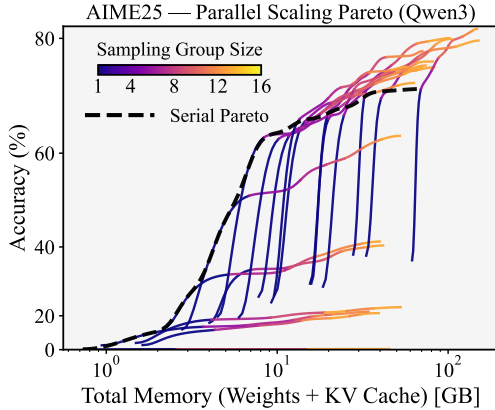


Figure 5: **Effect of parallel scaling on the Pareto frontier (Qwen3).** Each colored curve represents the Pareto frontier for a specific model size and weight precision, obtained by increasing the sampling group size,  $G$ . Pareto frontier for serial scaling ( $G = 1$ ) across all models is shown as the dotted line. Parallel scaling is only effective for large models.

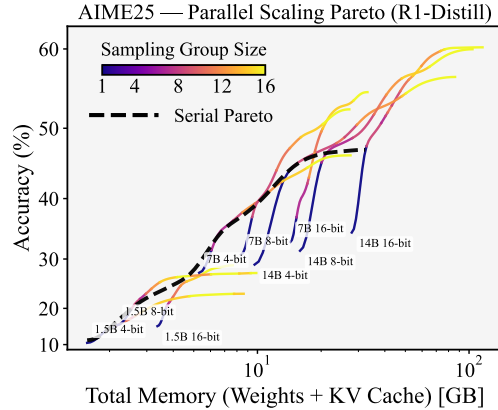


Figure 6: **Effect of parallel scaling on the Pareto frontier (DeepSeek-R1-Distill).** A similar scale-dependent pattern holds for DeepSeek-R1-Distill: parallel scaling is memory-inefficient for small models but improves the Pareto frontier for sufficiently large ones.

**The effectiveness of parallel scaling is scale-dependent.** For systematic evaluation, we use budget forcing to control the token budget for each of the  $G$  parallel samples and use majority voting to select the final answer. **This majority voting protocol corresponds to self-consistency with majority aggregation (Wang et al., 2022).** Figure 5 shows how parallel scaling affects the memory–accuracy trade-off. The dotted line marks the Pareto frontier from serial scaling alone. Each colored curve represents the frontier for a specific model configuration as the group size,  $G$ , is increased (see Appendix C.5, Figure 15 for a per-model breakdown). For models effectively smaller than 8-bit 4B, parallel scaling is memory-inefficient, as its configurations lie below the frontier established by serial scaling alone. However, for large models, parallel scaling improves the trade-off, and the memory-optimal group size  $G$  on the global Pareto frontier increases with the memory budget. While group sizes of  $4 \leq G < 8$  are memory-optimal in the 16.4–28.9 GB range, for budgets above 28.9 GB, the frontier is pushed by even larger groups ( $G \geq 8$ ). **This scale-dependent behavior is not unique to Qwen3: for DeepSeek-R1-Distill and OpenReasoning-Nemotron (Figures 6 and 16), parallel scaling is memory-inefficient for smaller effective sizes but improves the Pareto frontier once models are sufficiently large.** Appendix C.6 provides detailed results on these reasoning model families.

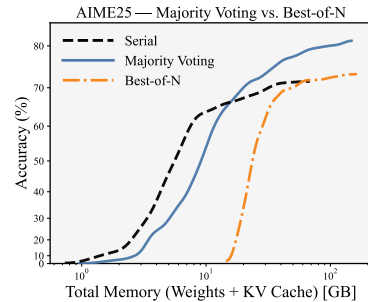
### Finding 3

For models effectively smaller than 8-bit 4B, serial scaling alone provides a better memory–accuracy trade-off than parallel scaling. For models effectively larger than this, parallel scaling improves the trade-off, and the memory-optimal group size  $G$  on the global Pareto frontier increases with the memory budget.

While this work focuses on memory trade-offs, practical scenarios also consider latency and throughput constraints. We analyze these trade-offs in Appendix C.1.

378 4.1 PARALLEL SCALING WITH AN EXTERNAL VERIFIER  
379

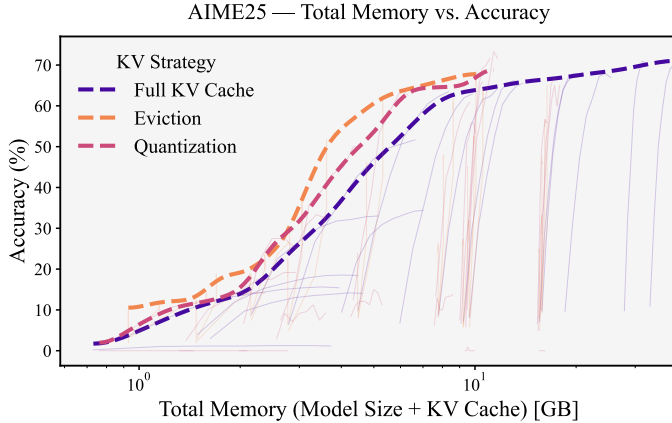
380 We evaluate Best-of-N parallel scaling with ActPRM-X (Duan  
381 et al., 2025) as an external PRM, accounting for its 7B (13.28  
382 GB) memory overhead in our total memory budget. Comparing  
383 the Pareto frontiers formed by serial scaling, majority-vote  
384 parallel scaling, and PRM-based Best-of-N (Figure 7), we find  
385 that the external verifier is consistently memory-inefficient:  
386 accuracy gains are marginal relative to the substantial fixed  
387 memory cost, and in low-memory regimes it can even under-  
388 perform serial scaling. These results suggest that under tight  
389 memory budgets, self-contained strategies such as majority  
390 voting are preferable to relying on large external verifiers.

391 Figure 7: **Parallel scaling with**  
392 **Best-of-N using ActPRM-X.**393 5 TEST-TIME SCALING WITH WEIGHT AND KV CACHE COMPRESSION  
394

395 Our analysis so far shows that while allocating more tokens generally improves accuracy, it is not  
396 always memory-efficient, especially for effectively small models where the KV cache can domi-  
397 nate total memory. While compressing the KV cache via quantization or eviction can reduce this  
398 footprint, it comes at a potential accuracy cost. This raises the following question:

399 *How do KV cache compression strategies, eviction, and quantization, alter the overall  
400 memory-accuracy trade-off, and which approach leads to stronger reasoning?*

401 To answer this, we evaluate both compression strategies across model sizes and weight precisions.  
402 For eviction, we use R-KV with target KV budgets of 8k, 4k, and 2k tokens. For KV cache quanti-  
403 zation, we use symmetric per-channel quantization to 8, 4, and 2-bit precisions with a group size of  
404 64 and a full-precision residual buffer of 128 tokens. The results are averaged over 8 generations per  
405 instance. We first show that both methods are broadly beneficial and then provide a detailed analysis  
406 to determine which strategy is optimal under different conditions.

422 Figure 8: **Memory vs. Accuracy by KV cache compression strategy (AIME25, Qwen3).** The  
423 plot shows the Pareto frontiers of KV cache compression across model sizes and weight precisions  
424 under serial scaling with budget forcing. Eviction uses R-KV with token budgets of 8k, 4k, and  
425 2k. Quantization is symmetric per-channel (group size 64) at 8-, 4-, and 2-bits. Faint background  
426 lines show curves for individual (model size, weight precision, KV strategy) configurations. Both  
427 compression strategies consistently improve the memory-accuracy trade-off.

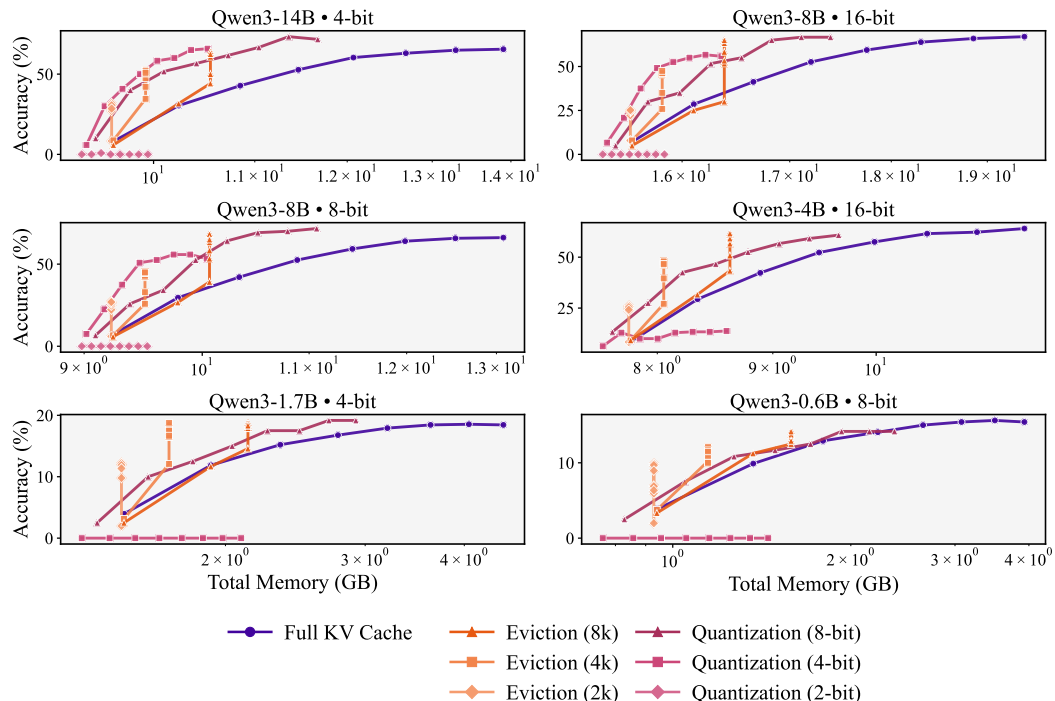
428 **KV cache eviction and quantization consistently advance the Pareto frontier across all tested**  
429 **model sizes and weight precisions.** Our first key finding, illustrated in Figure 8, is that the aggre-  
430 **gated Pareto frontiers for both quantization and eviction decisively advance beyond a baseline without**

432 compression for models with 4-bit, 8-bit, and 16-bit weights. This improvement demonstrates that  
 433 these strategies enable either higher accuracy at the same memory budget or the same accuracy  
 434 at a lower memory cost, regardless of the model weight precision. The benefits are especially pro-  
 435 nounced in the low-memory regime below 10 GB, where smaller models are most constrained by the  
 436 KV cache. This indicates that even when model weights are aggressively compressed, the KV cache  
 437 contains significant redundancies that can be exploited. Our results, therefore, establish KV cache  
 438 compression as an essential and broadly beneficial strategy for the memory-efficient deployment of  
 439 reasoning models.

440 **Finding 4**

442 Weight quantization alone is not sufficient for memory-optimal reasoning. KV cache com-  
 443 pression advances the memory–accuracy frontier across all weight precisions.  
 444

445 Having established that KV cache compression is broadly beneficial, we now analyze which com-  
 446 pression strategy, quantization or eviction, is preferable for a given model size  $N$  and weight pre-  
 447 cision  $P_W$ . Figure 9 shows the resulting memory–accuracy trade-offs, where each strategy shapes  
 448 the curves differently. Quantization reduces the memory cost per token, shifting the curves leftward,  
 449 typically with some accuracy degradation. Eviction, in contrast, enforces a fixed memory ceiling  
 450 for the KV cache, resulting in characteristic vertical curves where accuracy improves while memory  
 451 usage remains constant.



476 **Figure 9: Per-model Memory vs. Accuracy by KV cache strategy (AIME25).** Each plot illus-  
 477 trates the memory–accuracy trade-off for a single model size and weight precision, comparing a full  
 478 KV cache baseline against R-KV eviction and symmetric per-channel quantization. Points along  
 479 each curve represent increasing number of processed tokens via budget forcing.  
 480  
 481

482 **Eviction is more effective than quantization for small models.** For models with an effective size  
 483 smaller than an 8-bit 8B model, eviction consistently provides the best memory–accuracy trade-off.  
 484 As shown in Figure 9 for the full-precision 4B model, eviction with an 8k token budget maintains  
 485 nearly lossless in maximum accuracy while substantially reducing total memory. This observation  
 486 holds across all weight precisions for the 4B model (see Appendix C.7, Figure 18 for these results).

486 In contrast, aggressive 4-bit KV cache quantization causes a significant drop in accuracy at these  
 487 small effective sizes. This suggests that effectively small models are more sensitive to the numerical  
 488 errors introduced by quantization, whereas eviction preserves the full precision of a smaller, more  
 489 critical set of tokens. For instance, on the 1.7B model with 4-bit weight precision, eviction achieves  
 490 the best memory trade-off while maintaining high accuracy, whereas an 8-bit quantized KV cache,  
 491 while effective, requires significantly more memory to reach a similar performance level.  
 492

493 **Quantization becomes competitive with eviction for large models.** For models with an effective  
 494 size larger than an 8-bit 8B model, the clear advantage of eviction diminishes as quantization be-  
 495 comes a highly competitive strategy. On the 8B model with 16-bit weights, for example, quantization  
 496 and eviction achieve comparable memory–accuracy trade-offs. While 4-bit KV cache quantization  
 497 is competitive, eviction with smaller budgets (4k or 2k) offers a similar trade-off in low-memory  
 498 regimes. This suggests that large models, with their greater number of effective parameters, are  
 499 more robust to the precision loss from quantization. However, we find that more aggressive 2-bit  
 500 quantization still results in a significant loss of accuracy.  
 501

### Finding 5

502 KV cache eviction provides a better memory–accuracy trade-off than KV cache quantization  
 503 for models with an effective size smaller than an 8-bit 8B model. For models at or above this  
 504 threshold, quantization becomes an increasingly competitive strategy.  
 505

## 6 CONCLUSION

506 Under real-world circumstances with fixed memory budgets, deploying reasoning models is ulti-  
 507 mately a problem of *where* to spend bytes, and practitioners are presented with a myriad of choices.  
 508 Our work reformulates test-time scaling around this constraint. We study the trade-offs in allocating  
 509 memory across model size, weight precision, KV cache compression, token budget, and sampling  
 510 group size for reasoning models. We find that the memory-optimal inference strategy for reason-  
 511 ing models *cannot be a one-size-fits-all prescription*: instead, it depends on the model’s capacity  
 512 (determined by effective size) and the nature of the task.  
 513

514 For smaller model sizes (typically models under the 8B size), prioritizing model weights yields  
 515 better memory–accuracy trade-offs by using higher-precision 8-/16-bit weights for mathematical  
 516 reasoning and favoring KV cache eviction over quantization. For larger models, increasing the token  
 517 budget until saturation and leveraging parallel scaling become the dominant strategies. Importantly,  
 518 the inflection point where extra KV cache beats extra model weight may change as models become  
 519 more sophisticated. However, by shifting the focus from FLOPs-based test-time scaling laws to  
 520 practical memory constraints, our framework and analysis provide general principles on how to  
 521 deploy reasoning models effectively.  
 522

## 7 LIMITATIONS AND FUTURE WORK

523 Our scope is intentionally focused to keep the search space tractable and inference-only. For test-  
 524 time scaling, we rely on prompt injection for serial scaling and majority voting for parallel scaling,  
 525 and only include a limited evaluation of an external verifier rather than a comprehensive compar-  
 526 ison of verifier-based methods. We compare a small set of post-training quantization schemes but  
 527 do not systematically study alternative KV cache eviction algorithms or training-time approaches  
 528 such as quantization-aware training. Our main analysis centers on the Qwen3 family, chosen for its  
 529 broad size range and fixed architecture, and two challenging benchmarks (AIME25 for mathemati-  
 530 cal reasoning and GPQA-Diamond for knowledge-intensive reasoning). However, additional exper-  
 531 iments on the DeepSeek-R1-Distill and OpenReasoning-Nemotron model families and on the Live-  
 532 CodeBench and MATH500 benchmarks suggest that our findings generalize beyond a single model  
 533 family and a single pair of benchmarks. These choices were necessary to maintain a tractable search  
 534 space, which already spans over 1,700 experimental configurations, and focus on self-contained  
 535 inference strategies, leaving a broader comparison of methods as a clear avenue for future work.  
 536

## 540 REFERENCES

541

542 AIME. AIME Problems and Solutions. [https://artofproblemsolving.com/wiki/index.php/AIME\\_Problems\\_and\\_Solutions](https://artofproblemsolving.com/wiki/index.php/AIME_Problems_and_Solutions), 2025.

543

544 Zeyuan Allen-Zhu and Yuanzhi Li. Physics of language models: Part 3.3, knowledge capacity  
545 scaling laws. *arXiv preprint arXiv:2404.05405*, 2024.

546

547 Hicham Badri and Appu Shaji. Half-quadratic quantization of large machine learning models,  
548 November 2023. URL [https://mobiusml.github.io/hqq\\_blog/](https://mobiusml.github.io/hqq_blog/).

549

550 Bradley Brown, Jordan Juravsky, Ryan Ehrlich, Ronald Clark, Quoc V Le, Christopher Ré, and  
551 Azalia Mirhoseini. Large language monkeys: Scaling inference compute with repeated sampling.  
552 *arXiv preprint arXiv:2407.21787*, 2024.

553

554 Zefan Cai, Wen Xiao, Hanshi Sun, Cheng Luo, Yikai Zhang, Ke Wan, Yucheng Li, Yeyang Zhou, Li-  
555 Wen Chang, Jiuxiang Gu, et al. R-kv: Redundancy-aware kv cache compression for training-free  
556 reasoning models acceleration. *arXiv preprint arXiv:2505.24133*, 2025.

557

558 Jerry Chee, Yaohui Cai, Volodymyr Kuleshov, and Christopher M De Sa. Quip: 2-bit quantization  
559 of large language models with guarantees. *Advances in Neural Information Processing Systems*,  
560 36:4396–4429, 2023.

561

562 Gheorghe Comanici, Eric Bieber, Mike Schaeckermann, Ice Pasupat, Noveen Sachdeva, Inderjit  
563 Dhillon, Marcel Blstein, Ori Ram, Dan Zhang, Evan Rosen, et al. Gemini 2.5: Pushing the  
564 frontier with advanced reasoning, multimodality, long context, and next generation agentic capa-  
565 bilities. *arXiv preprint arXiv:2507.06261*, 2025.

566

567 Tri Dao. Flashattention-2: Faster attention with better parallelism and work partitioning. *arXiv  
568 preprint arXiv:2307.08691*, 2023.

569

570 Tim Dettmers and Luke Zettlemoyer. The case for 4-bit precision: k-bit inference scaling laws. In  
571 *International Conference on Machine Learning*, pp. 7750–7774. PMLR, 2023.

572

573 Tim Dettmers, Mike Lewis, Younes Belkada, and Luke Zettlemoyer. Gpt3. int8 (): 8-bit matrix  
574 multiplication for transformers at scale. *Advances in neural information processing systems*, 35:  
575 30318–30332, 2022.

576

577 Keyu Duan, Zichen Liu, Xin Mao, Tianyu Pang, Changyu Chen, Qiguang Chen, Michael Qizhe  
578 Shieh, and Longxu Dou. Efficient process reward model training via active learning. *arXiv  
579 preprint arXiv:2504.10559*, 2025.

580

581 Guhao Feng, Kai Yang, Yuntian Gu, Xinyue Ai, Shengjie Luo, Jiacheng Sun, Di He, Zhenguo Li,  
582 and Liwei Wang. How numerical precision affects arithmetical reasoning capabilities of llms. In  
583 *Findings of the Association for Computational Linguistics: ACL 2025*, pp. 46–85, 2025.

584

585 Elias Frantar, Saleh Ashkboos, Torsten Hoefer, and Dan Alistarh. Gptq: Accurate post-training  
586 quantization for generative pre-trained transformers. *arXiv preprint arXiv:2210.17323*, 2022.

587

588 Samir Yitzhak Gadre, Georgios Smyrnis, Vaishaal Shankar, Suchin Gururangan, Mitchell Worts-  
589 man, Rulin Shao, Jean Mercat, Alex Fang, Jeffrey Li, Sedrick Keh, et al. Language models scale  
590 reliably with over-training and on downstream tasks. In *The Thirteenth International Conference  
591 on Learning Representations*, 2025.

592

593 Suyu Ge, Yunan Zhang, Liyuan Liu, Minjia Zhang, Jiawei Han, and Jianfeng Gao. Model tells  
594 you what to discard: Adaptive kv cache compression for llms. *arXiv preprint arXiv:2310.01801*,  
595 2023.

596

597 Daya Guo, Dejian Yang, Haowei Zhang, Junxiao Song, Ruoyu Zhang, Runxin Xu, Qihao Zhu,  
598 Shirong Ma, Peiyi Wang, Xiao Bi, et al. Deepseek-r1: Incentivizing reasoning capability in llms  
599 via reinforcement learning. *arXiv preprint arXiv:2501.12948*, 2025.

600

601 Tom Henighan, Jared Kaplan, Mor Katz, Mark Chen, Christopher Hesse, Jacob Jackson, Heewoo  
602 Jun, Tom B Brown, Prafulla Dhariwal, Scott Gray, et al. Scaling laws for autoregressive generative  
603 modeling. *arXiv preprint arXiv:2010.14701*, 2020.

594 Jordan Hoffmann, Sebastian Borgeaud, Arthur Mensch, Elena Buchatskaya, Trevor Cai, Eliza  
 595 Rutherford, Diego de Las Casas, Lisa Anne Hendricks, Johannes Welbl, Aidan Clark, et al. Training  
 596 compute-optimal large language models. *arXiv preprint arXiv:2203.15556*, 2022.

597

598 Coleman Hooper, Sehoon Kim, Hiva Mohammadzadeh, Michael W Mahoney, Yakun S Shao, Kurt  
 599 Keutzer, and Amir Gholami. Kvquant: Towards 10 million context length lilm inference with kv  
 600 cache quantization. *Advances in Neural Information Processing Systems*, 37:1270–1303, 2024.

601

602 Aaron Jaech, Adam Kalai, Adam Lerer, Adam Richardson, Ahmed El-Kishky, Aiden Low, Alec  
 603 Helyar, Aleksander Madry, Alex Beutel, Alex Carney, et al. Openai o1 system card. *arXiv  
 604 preprint arXiv:2412.16720*, 2024.

605

606 Naman Jain, King Han, Alex Gu, Wen-Ding Li, Fanjia Yan, Tianjun Zhang, Sida Wang, Armando  
 607 Solar-Lezama, Koushik Sen, and Ion Stoica. Livecodebench: Holistic and contamination free  
 608 evaluation of large language models for code. *arXiv preprint arXiv:2403.07974*, 2024.

609

610 Hao Kang, Qingru Zhang, Souvik Kundu, Geonhwa Jeong, Zaoxing Liu, Tushar Krishna, and Tuo  
 611 Zhao. Gear: An efficient kv cache compression recipe for near-lossless generative inference of  
 612 lilm. *arXiv preprint arXiv:2403.05527*, 2024.

613

614 Jared Kaplan, Sam McCandlish, Tom Henighan, Tom B Brown, Benjamin Chess, Rewon Child,  
 615 Scott Gray, Alec Radford, Jeffrey Wu, and Dario Amodei. Scaling laws for neural language  
 616 models. *arXiv preprint arXiv:2001.08361*, 2020.

617

618 Junhyuck Kim, Jongho Park, Jaewoong Cho, and Dimitris Papailiopoulos. Lexico: Extreme kv  
 619 cache compression via sparse coding over universal dictionaries. In *Forty-second International  
 620 Conference on Machine Learning*, 2024.

621

622 Sehoon Kim, Coleman Hooper, Amir Gholami, Zhen Dong, Xiuyu Li, Sheng Shen, Michael W  
 623 Mahoney, and Kurt Keutzer. Squeezellm: Dense-and-sparse quantization. *arXiv preprint  
 624 arXiv:2306.07629*, 2023.

625

626 Tanishq Kumar, Zachary Ankner, Benjamin F Spector, Blake Bordelon, Niklas Muennighoff, Man-  
 627 sheej Paul, Cengiz Pehlevan, Christopher Ré, and Aditi Raghunathan. Scaling laws for precision.  
 628 *arXiv preprint arXiv:2411.04330*, 2024.

629

630 Woosuk Kwon, Zuhuan Li, Siyuan Zhuang, Ying Sheng, Lianmin Zheng, Cody Hao Yu, Joseph  
 631 Gonzalez, Hao Zhang, and Ion Stoica. Efficient memory management for large language model  
 632 serving with pagedattention. In *Proceedings of the 29th Symposium on Operating Systems Prin-  
 633 ciples*, pp. 611–626, 2023.

634

635 Yuhong Li, Yingbing Huang, Bowen Yang, Bharat Venkitesh, Acyr Locatelli, Hanchen Ye, Tianle  
 636 Cai, Patrick Lewis, and Deming Chen. Snapkv: Lilm knows what you are looking for before  
 637 generation. *Advances in Neural Information Processing Systems*, 37:22947–22970, 2024.

638

639 Zhen Li, Yupeng Su, Runming Yang, Congkai Xie, Zheng Wang, Zhongwei Xie, Ngai Wong, and  
 640 Hongxia Yang. Quantization meets reasoning: Exploring lilm low-bit quantization degradation for  
 641 mathematical reasoning. *arXiv preprint arXiv:2501.03035*, 2025a.

642

643 Zhong-Zhi Li, Duzhen Zhang, Ming-Liang Zhang, Jiaxin Zhang, Zengyan Liu, Yuxuan Yao, Haotian  
 644 Xu, Junhao Zheng, Pei-Jie Wang, Xiuyi Chen, et al. From system 1 to system 2: A survey of  
 645 reasoning large language models. *arXiv preprint arXiv:2502.17419*, 2025b.

646

647 Hunter Lightman, Vineet Kosaraju, Yuri Burda, Harrison Edwards, Bowen Baker, Teddy Lee, Jan  
 648 Leike, John Schulman, Ilya Sutskever, and Karl Cobbe. Let’s verify step by step. In *The Twelfth  
 649 International Conference on Learning Representations*, 2023.

650

651 Ji Lin, Jiaming Tang, Haotian Tang, Shang Yang, Wei-Ming Chen, Wei-Chen Wang, Guangxuan  
 652 Xiao, Xingyu Dang, Chuang Gan, and Song Han. Awq: Activation-aware weight quantization  
 653 for on-device lilm compression and acceleration. *Proceedings of machine learning and systems*,  
 654 6:87–100, 2024.

648 Ruijang Liu, Yuxuan Sun, Manyi Zhang, Haoli Bai, Xianzhi Yu, Tiezheng Yu, Chun Yuan, and  
 649 Lu Hou. Quantization hurts reasoning? an empirical study on quantized reasoning models. *arXiv*  
 650 *preprint arXiv:2504.04823*, 2025a.

651

652 Zechun Liu, Barlas Oguz, Changsheng Zhao, Ernie Chang, Pierre Stock, Yashar Mehdad, Yangyang  
 653 Shi, Raghuraman Krishnamoorthi, and Vikas Chandra. Llm-qat: Data-free quantization aware  
 654 training for large language models. *arXiv preprint arXiv:2305.17888*, 2023a.

655 Zechun Liu, Changsheng Zhao, Hanxian Huang, Sijia Chen, Jing Zhang, Jiawei Zhao, Scott Roy,  
 656 Lisa Jin, Yunyang Xiong, Yangyang Shi, et al. Paretoq: Scaling laws in extremely low-bit llm  
 657 quantization. *arXiv preprint arXiv:2502.02631*, 2025b.

658

659 Zichang Liu, Aditya Desai, Fangshuo Liao, Weitao Wang, Victor Xie, Zhaozhuo Xu, Anastasios  
 660 Kyrillidis, and Anshumali Shrivastava. Scissorhands: Exploiting the persistence of importance  
 661 hypothesis for llm kv cache compression at test time. *Advances in Neural Information Processing*  
 662 *Systems*, 36:52342–52364, 2023b.

663

664 Zirui Liu, Jiayi Yuan, Hongye Jin, Shaochen Zhong, Zhaozhuo Xu, Vladimir Braverman, Beidi  
 665 Chen, and Xia Hu. Kivi: A tuning-free asymmetric 2bit quantization for kv cache. *arXiv preprint*  
 666 *arXiv:2402.02750*, 2024.

667 Shuming Ma, Hongyu Wang, Lingxiao Ma, Lei Wang, Wenhui Wang, Shaohan Huang, Lifeng Dong,  
 668 Ruiping Wang, Jilong Xue, and Furu Wei. The era of 1-bit llms: All large language models are in  
 669 1.58 bits. *arXiv preprint arXiv:2402.17764*, 1, 2024.

670 Somshubra Majumdar, Igor Gitman, Shubham Toshniwal, and Aleksander. Openreasoning-  
 671 nemotron: A family of state-of-the-art distilled reasoning models. <https://huggingface.co/blog/nvidia/openreasoning-nemotron>, 2025. Hugging Face community article.

672

673 Anmol Mekala, Anirudh Atmakuru, Yixiao Song, Marzena Karpinska, and Mohit Iyyer. Does quan-  
 674 tization affect models' performance on long-context tasks? *arXiv preprint arXiv:2505.20276*,  
 675 2025.

676

677 Paulius Micikevicius, Dusan Stosic, Neil Burgess, Marius Cornea, Pradeep Dubey, Richard Grisen-  
 678 thwaite, Sangwon Ha, Alexander Heinecke, Patrick Judd, John Kamalu, et al. Fp8 formats for  
 679 deep learning. *arXiv preprint arXiv:2209.05433*, 2022.

680

681 John X Morris, Chawin Sitawarin, Chuan Guo, Narine Kokhlikyan, G Edward Suh, Alexander M  
 682 Rush, Kamalika Chaudhuri, and Saeed Mahloujifar. How much do language models memorize?  
 683 *arXiv preprint arXiv:2505.24832*, 2025.

684

685 Niklas Muennighoff, Zitong Yang, Weijia Shi, Xiang Lisa Li, Li Fei-Fei, Hannaneh Hajishirzi, Luke  
 686 Zettlemoyer, Percy Liang, Emmanuel Candès, and Tatsunori Hashimoto. s1: Simple test-time  
 687 scaling. *arXiv preprint arXiv:2501.19393*, 2025.

688

689 Qwen Team. Qwq-32b: Embracing the power of reinforcement learning, March 2025. URL  
<https://qwenlm.github.io/blog/qwq-32b/>.

690

691 David Rein, Betty Li Hou, Asa Cooper Stickland, Jackson Petty, Richard Yuanzhe Pang, Julien Di-  
 692 rani, Julian Michael, and Samuel R Bowman. Gpqa: A graduate-level google-proof q&a bench-  
 693 mark. In *First Conference on Language Modeling*, 2024.

694

695 Ranajoy Sadhukhan, Zhuoming Chen, Haizhong Zheng, Yang Zhou, Emma Strubell, and Beidi  
 696 Chen. Kinetics: Rethinking test-time scaling laws. In *ICML 2025 Workshop on Long-Context*  
 697 *Foundation Models*.

698

699 Charlie Snell, Jaehoon Lee, Kelvin Xu, and Aviral Kumar. Scaling llm test-time compute optimally  
 700 can be more effective than scaling model parameters. *arXiv preprint arXiv:2408.03314*, 2024.

701

Kimi Team, Angang Du, Bofei Gao, Bowei Xing, Changjiu Jiang, Cheng Chen, Cheng Li, Chenjun  
 Xiao, Chenzhuang Du, Chonghua Liao, et al. Kimi k1.5: Scaling reinforcement learning with  
 llms. *arXiv preprint arXiv:2501.12599*, 2025.

702 Jian Wang, Boyan Zhu, Chak Tou Leong, Yongqi Li, and Wenjie Li. Scaling over scaling: Exploring  
 703 test-time scaling pareto in large reasoning models. *arXiv preprint arXiv:2505.20522*, 2025.  
 704

705 Xuezhi Wang, Jason Wei, Dale Schuurmans, Quoc Le, Ed Chi, Sharan Narang, Aakanksha Chowdh-  
 706 ery, and Denny Zhou. Self-consistency improves chain of thought reasoning in language models.  
 707 *arXiv preprint arXiv:2203.11171*, 2022.

708 Jason Wei, Xuezhi Wang, Dale Schuurmans, Maarten Bosma, Fei Xia, Ed Chi, Quoc V Le, Denny  
 709 Zhou, et al. Chain-of-thought prompting elicits reasoning in large language models. *Advances in*  
 710 *Neural Information Processing Systems*, 35:24824–24837, 2022.

711 Yangzhen Wu, Zhiqing Sun, Shanda Li, Sean Welleck, and Yiming Yang. Inference scaling laws:  
 712 An empirical analysis of compute-optimal inference for problem-solving with language models.  
 713 *arXiv preprint arXiv:2408.00724*, 2024.

714

715 Guangxuan Xiao, Ji Lin, Mickael Seznec, Hao Wu, Julien Demouth, and Song Han. Smoothquant:  
 716 Accurate and efficient post-training quantization for large language models. In *International*  
 717 *Conference on Machine Learning*, pp. 38087–38099. PMLR, 2023a.

718 Guangxuan Xiao, Yuandong Tian, Beidi Chen, Song Han, and Mike Lewis. Efficient streaming  
 719 language models with attention sinks. *arXiv preprint arXiv:2309.17453*, 2023b.

720

721 An Yang, Anfeng Li, Baosong Yang, Beichen Zhang, Binyuan Hui, Bo Zheng, Bowen Yu,  
 722 Chang Gao, Chengan Huang, Chenxu Lv, et al. Qwen3 technical report. *arXiv preprint*  
 723 *arXiv:2505.09388*, 2025.

724

725 Zhewei Yao, Xiaoxia Wu, Cheng Li, Stephen Youn, and Yuxiong He. Zeroquant-v2: Exploring  
 726 post-training quantization in llms from comprehensive study to low rank compensation. *arXiv*  
 727 *preprint arXiv:2303.08302*, 2023.

728

729 Nan Zhang, Yusen Zhang, Prasenjit Mitra, and Rui Zhang. When reasoning meets compression:  
 730 Benchmarking compressed large reasoning models on complex reasoning tasks. *arXiv preprint*  
 731 *arXiv:2504.02010*, 2025.

732

733 Zhenyu Zhang, Ying Sheng, Tianyi Zhou, Tianlong Chen, Lianmin Zheng, Ruisi Cai, Zhao Song,  
 734 Yuandong Tian, Christopher Ré, Clark Barrett, et al. H2o: Heavy-hitter oracle for efficient gen-  
 735 erative inference of large language models. *Advances in Neural Information Processing Systems*,  
 736 36:34661–34710, 2023.

737

738 James Xu Zhao, Bryan Hooi, and See-Kiong Ng. Test-time scaling in reasoning models is not  
 739 effective for knowledge-intensive tasks yet. *arXiv preprint arXiv:2509.06861*, 2025.

740

741

742

743

744

745

746

747

748

749

750

751

752

753

754

755

756 A RELATED WORK  
757

758 **Train-time scaling and knowledge capacity.** Foundational scaling studies (Kaplan et al., 2020;  
759 Henighan et al., 2020; Hoffmann et al., 2022) establish power-law relationships between model size,  
760 data, and loss, yielding prescriptions for compute-optimal training under fixed compute budgets.  
761 While these results provide guidance for allocating parameters and tokens during pre-training, they  
762 do not consider inference-time compute and hence require new extrapolations (Gadre et al., 2025). In  
763 parallel, capacity-oriented analyses estimate what models can store, either by modeling knowledge  
764 as information per parameter or by measuring memorization versus generalization (Morris et al.,  
765 2025; Allen-Zhu & Li, 2024). These views motivate a budget-centric view but leave precision and  
766 inference-time trade-offs under deployment constraints unspecified. Bit-normalized studies examine  
767 how performance at different precision scales with total model bits (Dettmers & Zettlemoyer, 2023)  
768 or the amount of training data (Kumar et al., 2024), particularly in zero-shot or few-shot scenarios.  
769 Feng et al. (2025); Mekala et al. (2025) further show that reduced numerical precision can markedly  
770 impair arithmetic reasoning and long-context performance unless compensated by a larger model  
771 size, indicating interactions between precision, task structure, and context length.  
772

773 **Inference-time methods and scaling laws.** Chain-of-thought prompting elicits intermediate  
774 steps, and self-consistency improves performance by sampling diverse rationales and aggregating  
775 them via majority voting (Wei et al., 2022; Wang et al., 2022). Modern reasoning models are trained  
776 to generate substantially more tokens, yielding significant gains across benchmarks (Wang et al.,  
777 2022; Wei et al., 2022; Brown et al., 2024; Muennighoff et al., 2025; Guo et al., 2025; Yang et al.,  
778 2025; Comanici et al., 2025; Jaech et al., 2024; Qwen Team, 2025; Team et al., 2025). Test-time  
779 scaling laws study how performance changes with increased FLOPs, tokens, or number of genera-  
780 tions, comparing strategies such as majority voting, best-of-n, and verification-based search (Brown  
781 et al., 2024; Wu et al., 2024; Snell et al., 2024; Muennighoff et al., 2025; Sadhukhan et al.; Wang  
782 et al., 2025; Zhao et al., 2025). However, these studies do not capture the impact of compression  
783 techniques such as weight-only quantization, which reduces memory and latency without affecting  
784 FLOPs. Moreover, the effects of jointly compressing model weights and the KV cache on test-time  
785 scaling remain underexplored despite their practical importance.  
786

787 **Efficient inference.** Various strategies have been proposed to address challenges in LLM quanti-  
788 zation, particularly handling outliers (Frantar et al., 2022; Xiao et al., 2023a; Lin et al., 2024; Kim  
789 et al., 2023; Dettmers et al., 2022). Quantization-aware training extends this idea by training models  
790 with quantized weights in the forward pass (Liu et al., 2023a; Ma et al., 2024; Liu et al., 2025b).  
791 Post-training KV cache compression techniques can be categorized into eviction and quantization.  
792 Eviction methods selectively discard less important entries based on different criteria (Cai et al.,  
793 2025; Xiao et al., 2023b; Zhang et al., 2023; Liu et al., 2023b; Li et al., 2024; Ge et al., 2023), while  
794 quantization approaches reduce the precision of cached values (Badri & Shaji, 2023; Kang et al.,  
795 2024; Liu et al., 2024; Kim et al., 2024; Hooper et al., 2024).  
796

797 **Quantization and reasoning.** Recent work has also examined how compression and low-bit quan-  
798 tization affect reasoning. Li et al. (2025a) find that aggressive weight quantization notably harms  
799 mathematical reasoning at low precision, consistent with our observation that 4-bit precision is  
800 memory-inefficient for mathematical reasoning. Liu et al. (2025a) show that the impact varies by  
801 bit-width and model family, and Zhang et al. (2025) benchmark compressed reasoning models on  
802 complex tasks to chart accuracy under compression. Our work complements these studies by fram-  
803 ing the problem as selecting a memory-optimal strategy for reasoning, identifying a scale-dependent  
804 threshold for allocating memory between model weights and longer generations, and incorporating  
805 KV cache compression into this analysis.  
806  
807  
808  
809

---

810 **B MEMORY EQUATIONS AND SPECIFICATIONS**  
811

812 The total memory cost  $C_{\text{mem}}$  is the sum of the memory required for the model weights  $M_{\text{weights}}$   
813 and the KV cache  $M_{\text{kv}}$ .  
814

815 **Weight Memory.** The total memory footprint for weights is the sum of memory for the quantized  
816 and unquantized parameters. The general equation is  
817

818 
$$M_{\text{weights}} \approx \underbrace{\left( N_{\text{quant}} \cdot \frac{P_W}{8} + \frac{N_{\text{quant}} \cdot (P_S + P_Z)}{g_W} \right)}_{\text{Quantized Parameters}} + \underbrace{\left( N_{\text{unquant}} \cdot \frac{P_{\text{native}}}{8} \right)}_{\text{Unquantized Parameters}} \quad [\text{bytes}]$$
819  
820

821 where  $N_{\text{quant}}$  and  $N_{\text{unquant}}$  are the number of quantized and unquantized parameters, respectively,  
822  $P_W$  is the low-bit precision for weights,  $g_W$  is the group size,  $P_S$  and  $P_Z$  are the bit-widths for the  
823 scales and zero-points, and  $P_{\text{native}}$  is the native precision of the unquantized layers.  
824

825 In our specific setup using GPTQ, the large linear layers are quantized, while components such as  
826 the token embedding matrix, normalization layer weights, and the final language model head remain  
827 in native BF16 precision. For our experiments, we use a group size  $g_W = 128$ , a scale precision of  
828  $P_S = 16$  (FP16), and symmetric quantization, making the zero-point precision  $P_Z = 0$ .  
829

830 **KV Cache Memory.** Without compression, the KV cache memory is given by  
831

832 
$$M_{\text{kv}} = G \cdot T \cdot n_{\text{layers}} \cdot n_{\text{kv\_heads}} \cdot d_{\text{head}} \cdot 2 \cdot \frac{P_{\text{native}}}{8} \quad [\text{bytes}]$$
833

834 where  $G$  is the sampling group size,  $T$  is the number of tokens,  $n_{\text{layers}}$  is the number of layers,  
835  $n_{\text{kv\_heads}}$  is the number of Key/Value heads,  $d_{\text{head}}$  is the dimension per head, the factor of 2 accounts  
836 for both Key and Value tensors, and  $P_{\text{native}}$  is the native precision of the cache elements in bits (e.g.,  
16 for BF16).  
837

838 The memory cost is modified by different KV cache strategies:  
839

840 

- **Eviction:** This strategy reduces the number of tokens stored. The memory cost is

841

842 
$$M_{\text{kv}} = G \cdot \min(T, T_{\text{retain}}) \cdot n_{\text{layers}} \cdot n_{\text{kv\_heads}} \cdot d_{\text{head}} \cdot 2 \cdot \frac{P_{\text{native}}}{8}$$
843

844 where  $T_{\text{retain}}$  is the maximum number of tokens retained by the policy. In our experiments,  
845 we use R-KV and test  $T_{\text{retain}} \in \{8192, 4096, 2048\}$ .  
846

847 

- **Quantization:** This strategy reduces the precision but introduces overhead for quantization  
848 parameters. The cost is  
849

850 
$$M_{\text{kv}} = (G \cdot T \cdot n_{\text{layers}} \cdot n_{\text{kv\_heads}} \cdot d_{\text{head}} \cdot 2) \cdot \left( \frac{P_{\text{kv}}}{8} + \frac{1}{g_{\text{kv}}} \frac{P_S + P_Z}{8} \right)$$
851

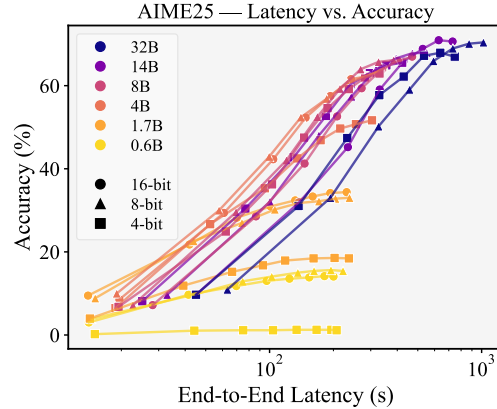
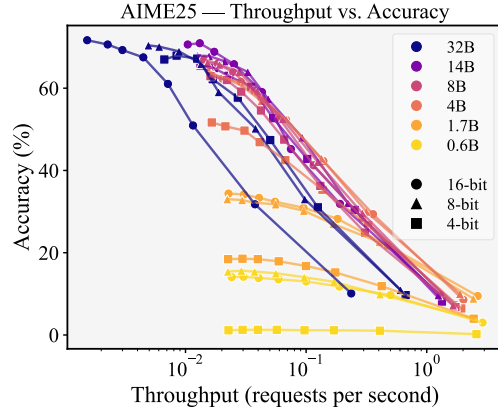
852 where  $g_{\text{kv}}$  is the group size, and  $P_S$  and  $P_Z$  are the precisions of the scales and zero-points.  
853 For our experiments, we use symmetric quantization ( $P_Z = 0$ ) with  $g_{\text{kv}} = 64$ ,  $P_S = 16$ ,  
854 and test  $P_{\text{kv}} \in \{8, 4, 2\}$ .  
855

856 Below are the architectural details and memory footprints for the models used in our experiments  
857 (Table 1).  
858

859  
860  
861  
862  
863

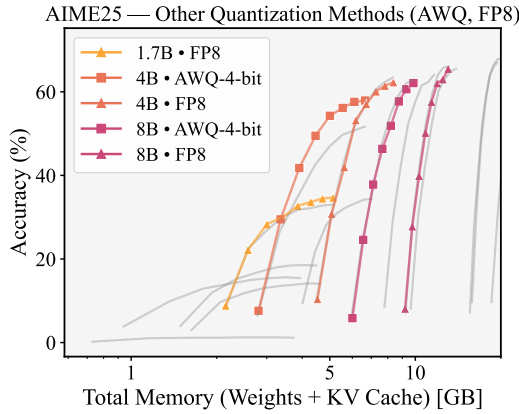
864  
865  
Table 1: Architectures and memory footprints of evaluated models.  
866  
867

Model	Model Size (GB)			$n_{\text{layers}}$	$n_{\text{kv.heads}}$	$d_{\text{head}}$	KV Cache (KB/token)
	4-bit	8-bit	16-bit				
Qwen3-0.6B	0.50	0.71	1.40	28	8	128	112
Qwen3-1.7B	1.26	1.93	3.78	28	8	128	112
Qwen3-4B	2.49	4.19	7.49	36	8	128	144
Qwen3-8B	5.68	8.94	15.26	36	8	128	144
Qwen3-14B	9.30	15.50	27.51	40	8	128	160
Qwen3-32B	18.01	32.66	61.02	64	8	128	256
R1-Distill/OpenReasoning-1.5B	1.51	2.12	3.31	28	2	128	28
R1-Distill/OpenReasoning-7B	5.19	8.25	14.19	28	4	128	56
R1-Distill/OpenReasoning-14B	9.30	15.50	27.51	48	8	128	192

868  
869  
870  
871  
872  
873  
874  
875  
C ADDITIONAL EXPERIMENTAL RESULTS876  
877  
878  
879  
C.1 LATENCY AND THROUGHPUT ANALYSIS880  
881 While we focus primarily on memory–accuracy trade-offs, latency and throughput can be important  
882 practical considerations as well. We analyze how model size, weight precision, and generation  
883 length affect both metrics.884  
885 **Experimental setup.** All measurements are performed on a single NVIDIA A100 80 GB GPU  
886 using the vLLM framework (Kwon et al., 2023) with FlashAttention (Dao, 2023) as the attention  
887 backend. To measure throughput for a given token budget, we sweep a range of batch sizes and  
888 record the highest batch size that completes successfully without out-of-memory errors or KV cache  
889 preemption.904  
905 Figure 10: **Latency vs. Accuracy trade-offs**  
906 **(AIME25, Qwen3).** Each curve shows end-to-  
907 end latency vs. accuracy for different model  
908 sizes and weight precisions with increasing  
909 generation length. Generation length emerges  
910 as the dominant factor in determining latency, with  
911 weight quantization providing more noticeable  
speedups for large models (14B, 32B).913 We show in Figure 10 that generation length is the dominant factor determining end-to-end latency  
914 across all model configurations. The benefit of weight quantization on latency due to reduced  
915 memory movement costs is modest for small models (up to 8B), but becomes noticeable for larger models  
916 (14B, 32B). For instance, the 14B model takes 137.7 seconds to generate 6k tokens at 16-bit preci-  
917 sion, while the 4-bit variant generates 10k tokens in 130.1 seconds. The 4B model with 8-bit and  
16-bit precision shows the strongest latency–accuracy trade-off.

918 The overall trend for throughput analysis in Figure 11 is similar to the latency findings. The 4B  
 919 model with 8-bit and 16-bit precision again demonstrates the strongest throughput–accuracy trade-  
 920 off, while the 32B model performs poorly due to slow generation and limited batch size scalability  
 921 under 80 GB VRAM constraints. Small size models (0.6B, 1.7B) achieve extreme batch sizes up to  
 922 160 and 170, respectively, yielding throughput of 2.9 and 2.64 requests per second with 2k token  
 923 generations. However, longer generations reduce maximum batch sizes and provide poor trade-offs  
 924 due to the fundamental accuracy limitations of these smaller models.

## C.2 RESULTS ON OTHER QUANTIZATION METHODS



922  
 923  
 924  
 925  
 926 **Figure 12: Comparison of quantization methods.** The background lines correspond to the GPTQ  
 927 curves from Figure 1. Memory–accuracy trade-offs remain consistent across different quantization  
 928 schemes.

929 To test whether our conclusions depend on a particular quantization scheme, we replicated the test-  
 930 time scaling analysis using AWQ (Lin et al., 2024) and FP8 (Micikevicius et al., 2022) quantization  
 931 on 1.7B, 4B, and 8B models. As shown in Figure 1, when plotted alongside GPTQ, the memory–  
 932 accuracy curves from AWQ and FP8 nearly overlap, confirming that the observed trend is not tied  
 933 to a specific quantization algorithm. Thus, the key memory-allocation pattern persists under these  
 934 schemes: at a low memory budget ( $\sim 4.1$  GB), a smaller FP8 1.7B model with a long 22k-token genera-  
 935 tion underperforms a larger AWQ-4-bit 4B model with a shorter 10k-token generation, whereas  
 936 at a higher budget ( $\sim 8$  GB), an FP8 4B model with 30k tokens outperforms an AWQ-4-bit 8B model  
 937 with 18k tokens. Overall, the AWQ and FP8 results reinforce our main conclusion that for smaller  
 938 effective sizes, memory is better spent on model weights, while for larger effective sizes it is better  
 939 spent on the KV cache to support longer generations.

### C.3 THEORETICAL BATCH SIZE ANALYSIS

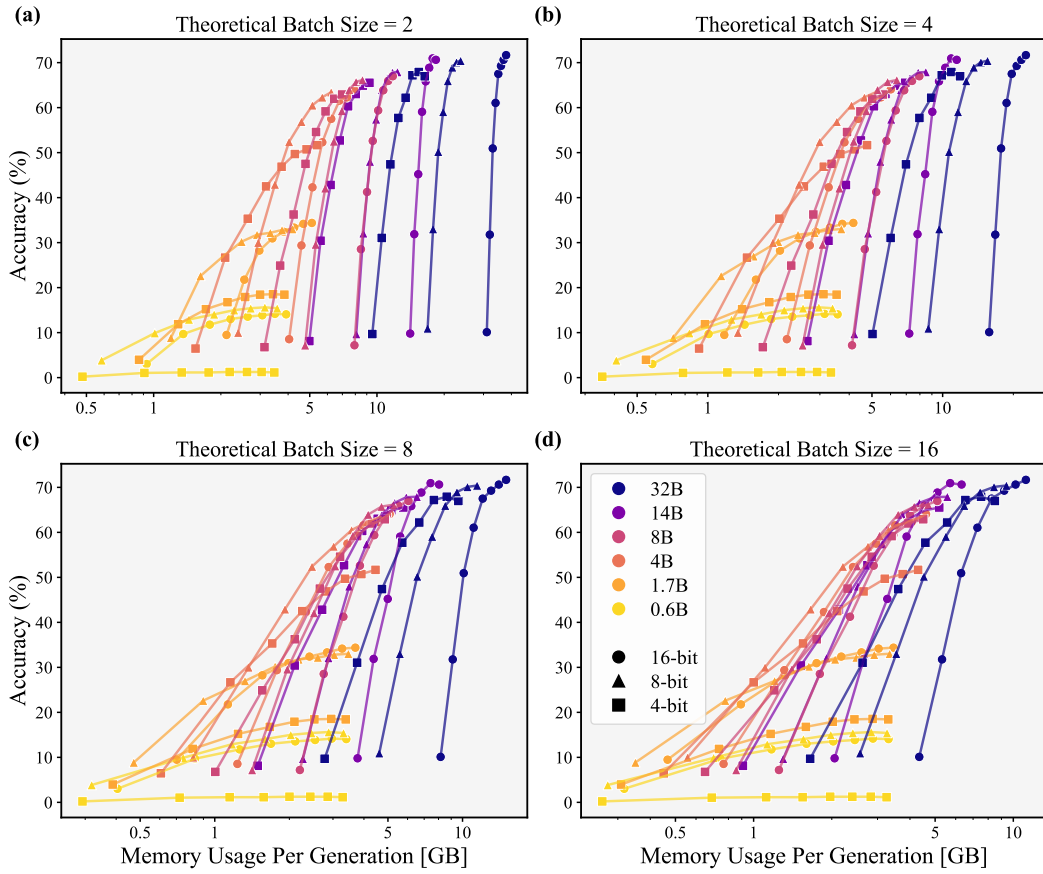


**Figure 13: Memory vs. Accuracy under different theoretical batch sizes (AIME25, Qwen3).** Each subplot shows memory-per-generation vs. accuracy for different theoretical batch sizes, where model weight memory is amortized across concurrent generations. The Pareto frontier shifts as batch size increases, revealing how model weight amortization affects the optimal memory allocation strategy.

Figure 13 examines how memory-accuracy trade-offs change when model weights are shared across multiple concurrent generations, as is common in production serving scenarios. As the theoretical batch size increases, the benefit of smaller model weights diminishes because weight costs are amortized across more generations. We find that the 0.6B model never appears on the Pareto frontier at a theoretical batch size of 16. The 8B and 14B models with 4-bit and 8-bit weight precision and the 4B model with 8-bit and 16-bit precision demonstrate favorable trade-offs in the 1–4 GB memory-per-generation region when the theoretical batch size is 16. Notably, the 8-bit 4B model consistently lies on the Pareto frontier for the 1–2 GB region.

1026  
1027

## C.4 DETAILED RESULTS ON LIVECODEBENCH AND MATH500

1028  
1029

To provide a more detailed view, we examine LiveCodeBench for code generation and MATH500 for a larger, more diverse set of math problems (Figure 3 and Figure 14).

1030  
1031  
1032  
1033  
1034  
1035  
1036  
1037  
1038

LiveCodeBench exhibits a trend very similar to AIME25. For models with an effective size below 8-bit 4B, allocating memory to model weights is superior. Under a low memory budget ( $\sim 6.2$  GB), a 4B 8-bit model with a 14k token budget achieves 61.7% accuracy, significantly outperforming a 1.7B 16-bit model with a larger 22k token budget, which only reaches 42.5%. Conversely, above the threshold, increasing the test-time budget becomes optimal. At a higher budget ( $\sim 10.5$  GB), a 4B 16-bit model with a 22k token budget reaches 65.00%, whereas a larger 14B 4-bit model with a restricted 6k token budget degrades to 26.8%. Notably, unlike the knowledge-intensive GPQA, 4-bit precision remains less memory-efficient on LiveCodeBench: a 16-bit 4B configuration is strictly more memory-efficient than a 4-bit 14B configuration.

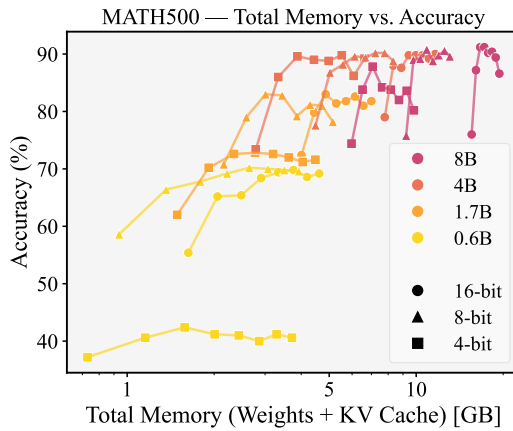
1039  
1040  
1041  
1042  
1043  
1044  
1045  
1046  
1047  
1048  
1049  
1050  
1051  
1052  
10531054  
1055  
1056  
1057

Figure 14: **Memory vs. Accuracy on MATH500 (Qwen3).** Serial scaling on MATH500 also exhibits a scale-dependent memory–accuracy trade-off, but the effective model size threshold shifts toward smaller models due to the benchmark’s relative ease.

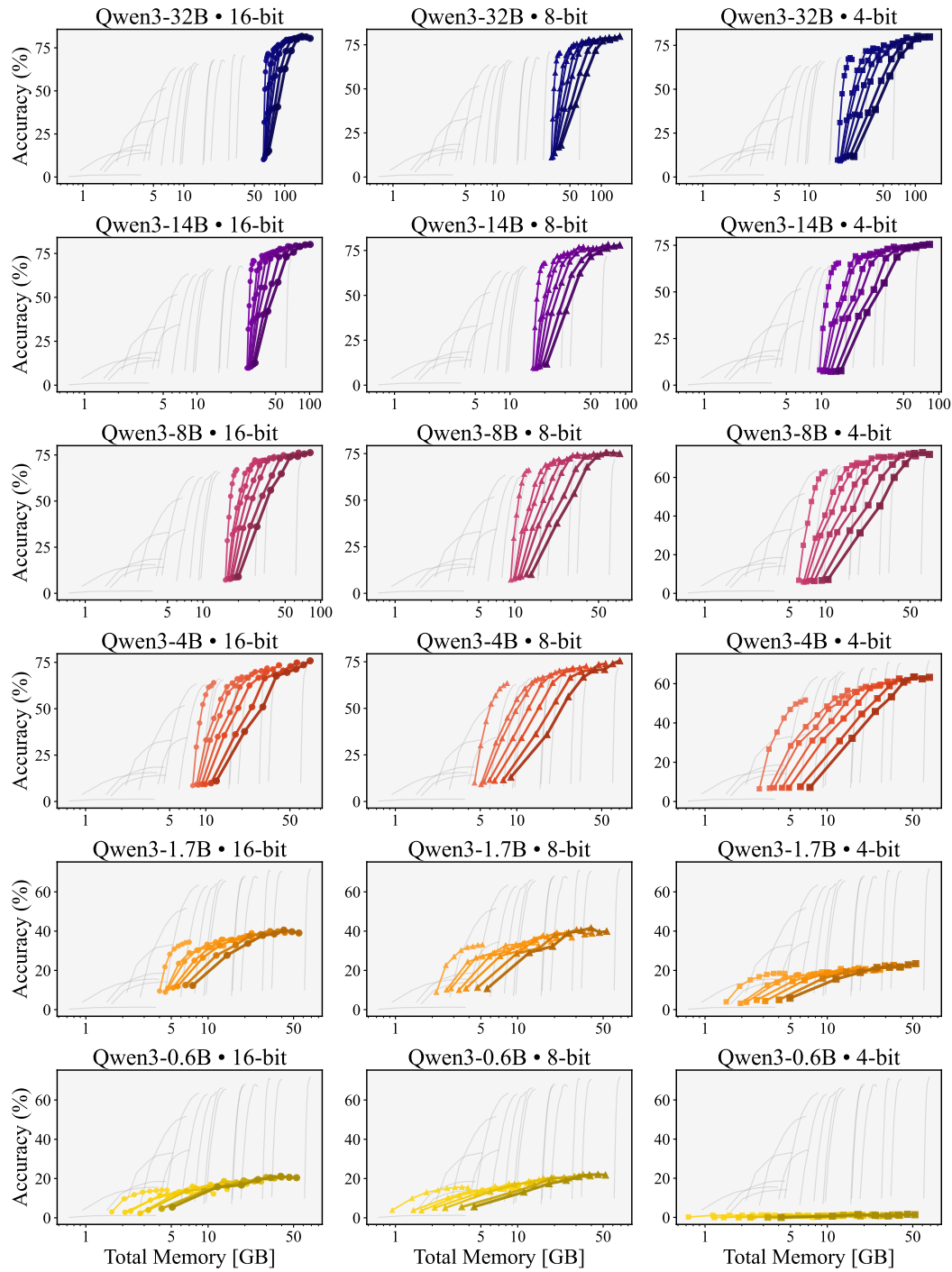
1058  
1059  
1060  
1061  
1062  
1063  
1064

For MATH500, the easier nature of the task shifts the threshold toward smaller effective sizes. Accuracy saturates quickly once models exceed roughly a 16-bit 1.7B effective size. However, below this threshold, investing in model weights remains more efficient. At a low memory budget ( $\sim 3.0$  GB), a 1.7B 8-bit model with a 10k token budget achieves 83.0%, outperforming a 0.6B 8-bit model with a 22k token budget at 70.0%. We also observe non-monotonicity in accuracy under budget forcing. This is because for an already-easy set, pushing generation length beyond what is needed can lead to reduced accuracy.

1065  
1066  
1067  
1068

Together, these results reinforce the existence of a scale-dependent threshold and the corresponding memory-optimal strategies. We also find that code generation as well as mathematical reasoning are sensitive to low-bit settings, and higher precision can be more memory-efficient than scaling to a larger model at 4-bit precision under a fixed budget.

1069  
1070  
1071  
1072  
1073  
1074  
1075  
1076  
1077  
1078  
1079

1080 C.5 DETAILED RESULTS FOR PARALLEL SCALING  
10811082 Figure 15 presents the per-model plots for the parallel scaling analysis discussed in Section 4.  
10831129 Figure 15: **Per-model Memory vs. Accuracy for parallel scaling (AIME25).** Each plot shows  
1130 the accuracy-memory trade-off for a single model and weight precision, comparing serial scaling  
1131 ( $G = 1$ ) with parallel scaling by increasing the sampling group size,  $G \in \{1, 3, 4, 6, 8, 12, 16\}$ .  
1132 Points along each curve represent increasing the token budget via budget forcing. Parallel scaling  
1133 improves the memory-accuracy trade-off, only for models effectively larger than 8-bit 4B.

1134  
1135

## C.6 DETAILED RESULTS ON OTHER MODEL FAMILIES

1136  
1137

To provide a more detailed view, we examine the DeepSeek-R1-Distill and OpenReasoning-Nemotron reasoning model families (Figures 6 and 16).

1138  
1139  
1140  
1141  
1142  
1143  
1144

For DeepSeek-R1-Distill on AIME25, under a low memory budget ( $\sim 9.6$  GB), allocating memory to model weights proves superior: a 7B 8-bit model with a 6k token KV cache ( $\sim 1.3$  GB) achieves 37.09% accuracy, significantly outperforming a 1.5B 8-bit model with a larger 18k token KV cache ( $G = 16$ ,  $\sim 7.8$  GB) which only reaches 27.60%. Conversely, in a high memory regime ( $\sim 30.1$  GB), allocating memory to the KV cache becomes optimal: a 7B 16-bit model with 18k tokens and parallel scaling ( $G = 16$ ) reaches 54.5%, surpassing a larger 14B 16-bit model with 14k tokens and serial scaling (39.2%).

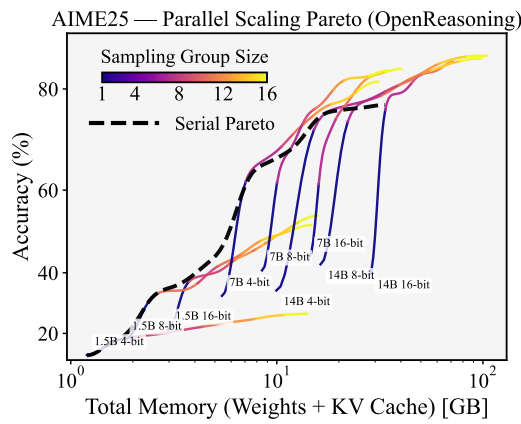
1145  
1146  
1147  
1148  
1149  
1150  
1151  
1152  
1153  
1154  
1155  
1156  
1157  
1158  
11591160  
1161  
1162

Figure 16: **Parallel scaling for OpenReasoning-Nemotron.** Comparison of serial vs. parallel scaling frontiers. Allocating substantial memory to the KV cache is only effective for sufficiently large models.

1163

Similar trends are observed for OpenReasoning-Nemotron. At a  $\sim 6.8$  GB budget, the 7B 4-bit model with 26k tokens ( $G = 1$ ) achieves 61.8%, outperforming the 1.5B 16-bit model with 18k tokens and parallel scaling ( $G = 8$ , 44.4%). At  $\sim 31.0$  GB, the 7B 16-bit model with 26k tokens and parallel scaling ( $G = 12$ ) reaches 81.1%, surpassing the 14B 16-bit model with 14k tokens (52.5%).

1164  
1165  
1166  
1167

These results confirm that the threshold behavior, favoring model weights for smaller effective sizes and KV cache for larger ones, is consistent across different reasoning model families, although the exact threshold may vary.

1168  
1169  
1170  
1171  
1172  
1173  
1174  
1175  
1176  
1177  
1178  
1179  
1180  
1181  
1182  
1183  
1184  
1185  
1186  
1187

1188  
1189

## C.7 DETAILED RESULTS FOR KV CACHE COMPRESSION

1190  
1191  
1192

Figures 17 and 18 show the per-model results for the KV cache compression analysis discussed in Section 5. For eviction, we also present results for StreamingLLM, where we retain the first  $T_{\text{retain}}/2$  tokens and the most recent  $T_{\text{retain}}/2$  tokens for a given retention budget  $T_{\text{retain}}$ .

1193

1194

1195

1196

1197

1198

1199

1200

1201

1202

1203

1204

1205

1206

1207

1208

1209

1210

1211

1212

1213

1214

1215

1216

1217

1218

1219

1220

1221

1222

1223

1224

1225

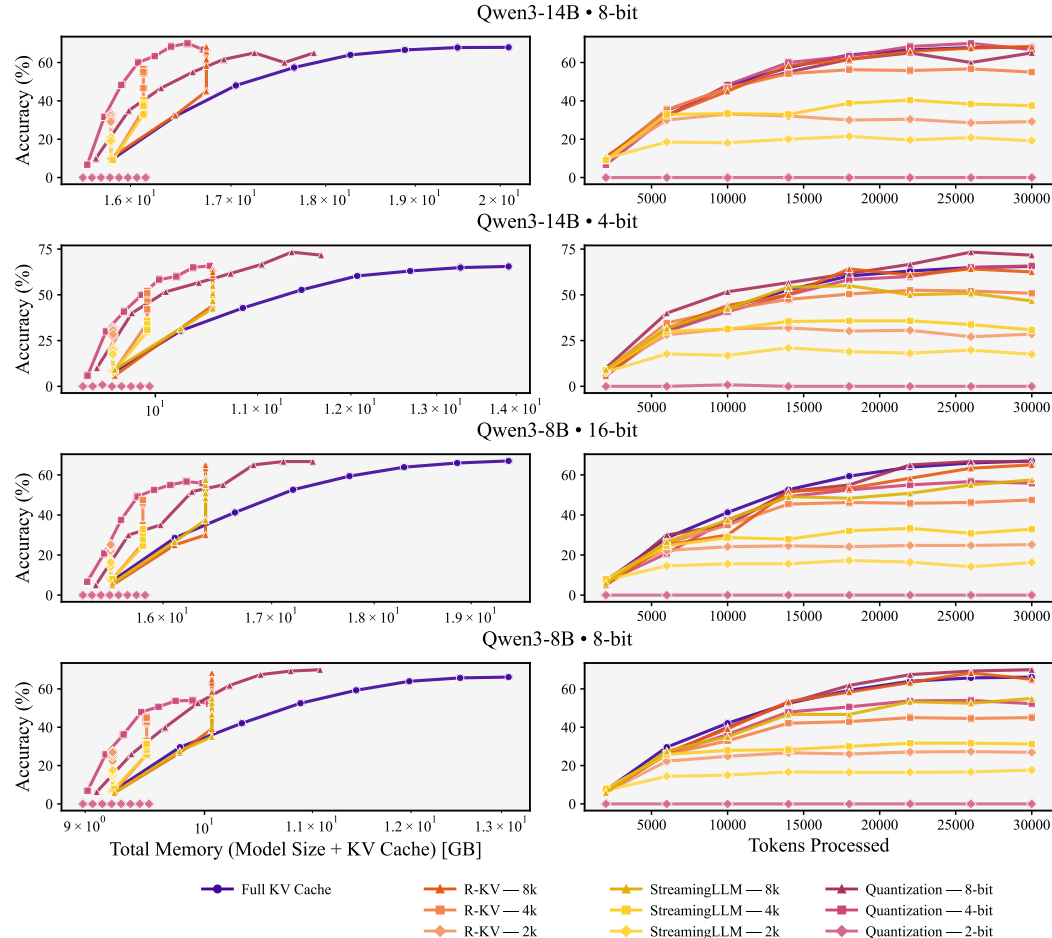


Figure 17: **Per-model Memory vs. Accuracy by KV cache strategy (AIME25, models > 4B).** Each plot shows the accuracy-memory trade-off for a single model and weight precision, comparing KV cache eviction methods (R-KV, StreamingLLM) against KV cache quantization and no compression. Points along each curve represent increasing the number of processed tokens.

1229

1230

1231

1232

1233

1234

1235

1236

1237

1238

1239

1240

1241

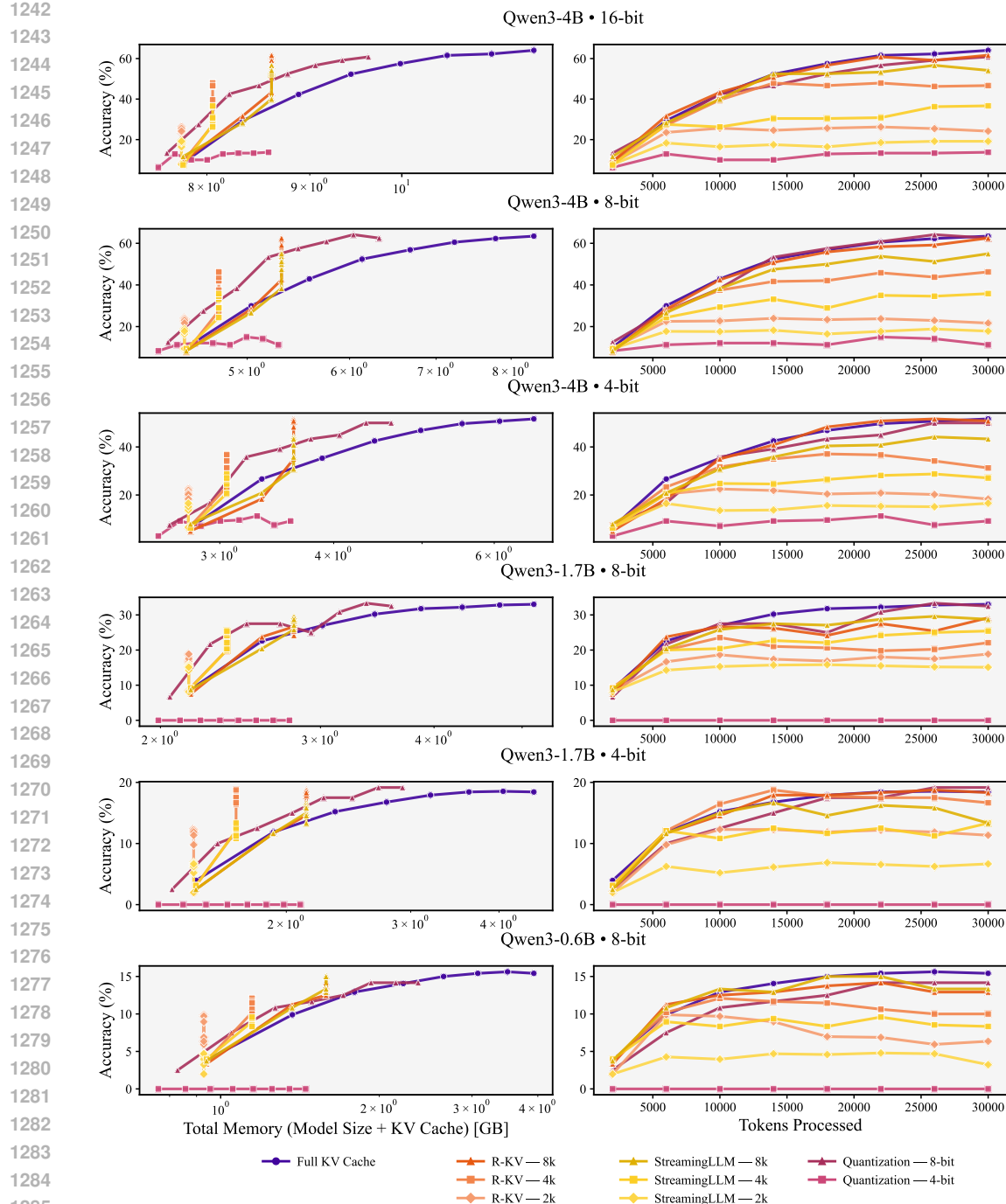


Figure 18: **Per-model Memory vs. Accuracy by KV cache strategy (AIME25, models  $\leq 4\text{B}$ ).** Each plot shows the accuracy-memory trade-off for a single model and weight precision, comparing KV cache eviction methods (R-KV, StreamingLLM) against KV cache quantization and no compression. Points along each curve represent increasing the number of processed tokens.